Articles

Cofactor-Induced Refolding: Refolding of Molten Globule Carbonic Anhydrase Induced by Zn(II) and Co(II)†

Dick Andersson, Per Hammarström,‡ and Uno Carlsson*

IFM-Department of Chemistry, Linköping University, SE-581 83 Linköping, Sweden

Received April 26, 2000; Revised Manuscript Received November 30, 2000

ABSTRACT: The stability versus unfolding to the molten globule intermediate of bovine carbonic anhydrase II (BCA II) in guanidine hydrochloride (GuHCl) was found to depend on the metal ion cofactor [Zn(II) or Co(II)], and the apoenzyme was observed to be least stable. Therefore, it was possible to find a denaturant concentration (1.2 M GuHCl) at which refolding from the molten globule to the native state could be initiated merely by adding the metal ion to the apo molten globule. Thus, refolding could be performed without changing the concentration of the denaturant. The molten globule intermediate of BCA II could still bind the metal cofactor. Cofactor-effected refolding from the molten globule to the native state can be summarized as follows: (1) initially, the metal ion binds to the molten globule; (2) compaction of the metal-binding site region is then induced by the metal ion binding; (3) a functioning active center is formed; and (4) finally, the native tertiary structure is generated in the outer parts of the protein.

The binding of metal ions to proteins has been studied extensively. The carbonic anhydrase metal-binding motif, with three His residues coordinating the metal ion [Zn(II)], has often been used to engineer novel metal-binding proteins (*1*). The aim of a metalloprotein-based design is to introduce new functions into naturally existing proteins or to increase the stability of an engineered or designed protein. The stability of bovine carbonic anhydrase II (BCA II),[1] for example, depends on the metal ion cofactor. The native state of Zn(II)-BCA II is more stable than that of Co(II)-BCA II, and the removal of the metal ion further destabilizes the native conformation (*2*, *3*). The Co(II)-enzyme has been observed in vitro to be almost as catalytically competent as the Zn(II)-enzyme (*4*).

BCA II is a Zn(II) enzyme that catalyzes the reversible hydration of CO_2, and the metal ion cofactor is essential for this function of the enzyme (*4*). The protein consists of a single polypeptide chain with a molecular mass of 29 kDa devoid of any sulfhydryl groups or disulfide bonds (*5*, *6*). The crystal structure of isoenzyme II has been determined for human but not for bovine CA. Isoenzymes from three different sources, namely, human CA I, human CA II, and bovine CA III, have all been found to exhibit very similar three-dimensional structures (*7*−*10*). It therefore is reasonable to assume that the fold does not differ much between BCA II and HCA II. Thus, the structure of BCA II should mainly be a β-sheet protein that is divided into two halves by 10 β-strands that penetrate the entire protein. One-half of the molecule should contain the N-terminal subdomain and the active site crevice, while the other half should include a large hydrophobic cluster. In HCA II, this hydrophobic core has been shown to be very resistant to unfolding (*11*−*13*). Furthermore, the metal ion in Co(II)-substituted HCA II has a tetrahedral coordination very similar to that of Zn(II) (*14*), and the coordinating histidines have been shown to move very little in the apoenzyme (*9*).

It has recently been demonstrated that the folding of several small proteins occurs via a two-stage process, while the folding of larger proteins often involves intermediates (*15*). The refolding of BCA II has been found to be remarkably complex, including both fast and slow kinetic stages, the slow stages being due to the isomerization of cis prolines in the unfolded and molten globule states of the protein (*16*−*18*). Furthermore, BCA II forms both equilibrium and kinetic molten globule intermediates (*19*). Because the stability of the native state of BCA II depends on the cofactor, lower concentrations of denaturant should be required to induce the molten globule state from the apoenzyme than from the Co(II)- and Zn(II)-enzymes. When the varying stabilities of the native and molten globule states of these protein forms are considered, perhaps a denaturant "window" could be found from which it might be possible to initiate formation of the native conformation from the molten globule state simply by adding the metal ion to the apoenzyme. By comparing the denaturation profiles of the apoenzyme and the holoenzymes, we found what we believed to be appropriate denaturing conditions (1.2 M GuHCl),

† Financial support of this work came from the Swedish Natural Science Research Council (U.C.), "Helge Ax:son Johnsons Stiftelse" (D.A. and P.H.), and "Stiftelsen Lars Hiertas Minne" (P.H.).

* To whom correspondence should be addressed.

‡ Present address: Department of Chemistry and Skaggs Institute for Chemical Biology, The Scripps Research Institute, 10550 N. Torrey Pines Rd., La Jolla, CA 92037.

[1] Abbreviations: ANS, 8-anilino-1-naphthalenesulfonic acid; BCA II, bovine carbonic anhydrase II; GuHCl, guanidine hydrochloride; HCA II, human carbonic anhydrase II.

10.1021/bi000957e CCC: $20.00
Published on Web 02/06/2001

under which such a refolding jump could be accomplished. Indeed, we were able to initiate refolding of the molten globule protein by adding equimolar concentrations of Zn(II) or Co(II).

Our aim with this work is also to shed light on the structural dynamics of the folding process, proceeding from the apo molten globule state to the native state of the holoenzyme [Zn(II)- and Co(II)-BCA II]. We felt that this approach would allow for the exploration of the role of the metal ion as well as its effects on the folding reaction. The refolding process was monitored by three methods, each probing a different aspect of the folding process: near-UV circular dichroism, intrinsic Trp fluorescence, and CO_2 hydration activity measurements.

MATERIALS AND METHODS

Chemicals. Guanidine hydrochloride (GuHCl; ultrapure), purchased from Chemicon, was determined to be metal-free by extraction with dithizone (7 mg/L) in carbon tetrachloride. The concentration of GuHCl was determined refractometrically (*20*). 8-Anilino-1-naphthalenesulfonic acid (ANS) was obtained from Sigma. All other chemicals were ultrapure or pro analysis grade.

Protein Purification and Preparation. BCA II was purified from cattle erythrocytes. Initial preparation and chromatographic conditions for purification of BCA II were like those of Lindskog (*21*), followed by affinity chromatography as described by Khalifah et al. (*22*). The purity of the enzyme was verified by sodium dodecyl sulfate−polyacrylamide gel electrophoresis. Protein concentrations were measured spectrophotometrically (Hitachi U2000 spectrophotometer) at 280 nm using an $A_{280}^{1\%}$ of 19.0 (*5*). The apoenzyme and the Zn(II)- and Co(II)-BCA II were prepared as described by Lindskog and Malmström (*23*), or as described by Hunt et al. (*24*). The proteins were prepared and stored in acid-cleaned (2 M HNO_3) plastic tubes. All utensils used during the experiments were made metal-free by soaking in 2 M HNO_3 for 2 days**,** and then by extensively rinsing with distilled water.

Equilibrium Unfolding. The stabilities of the enzyme forms were determined after incubation for 24 h at 23 °C in various concentrations of GuHCl buffered with 0.1 M Tris-H_2SO_4 (pH 7.5). The equilibrium unfolding transitions were monitored by near-UV CD spectroscopy [0.25 mg mL^{-1} (8.5 μM)] and intrinsic Trp fluorescence [0.025 mg mL^{-1} (0.85 μM)].

Kinetic Measurements. The kinetics of the refolding process were monitored by the following methods: near-UV CD (spectra and change in ellipticity at 270 nm), Trp fluorescence (change in intensity at 340 nm), and CO_2 hydration activity. Apo-BCA II [0.25 mg mL^{-1} $(8.5\ \mu M)^{-1}$] was incubated for 1 h in 1.20 M GuHCl buffered with 0.1 M Tris-H_2SO_4 (pH 7.5) at 23 °C. Refolding was initiated by manually mixing an equimolar amount of cofactor [Zn(II) or Co(II)] in a small volume (1.9 μL) to the apoenzyme (1.90 mL) to avoid dilution of the protein and denaturant. Each kinetic experiment was repeated at least three times. Reference samples containing Zn(II)- or Co(II)-BCA II instead of apo-BCA II were incubated under identical conditions (0 and 1.20 M GuHCl) so that the increase in activity (CO_2 hydration) and spectroscopic properties (near-UV CD and intrinsic fluorescence) could be monitored during the refolding process.

Enzymatic Activity Measurements. CO_2 hydration activity was determined according to the method of Rickli et al. (*25*). Ethylenediaminetetraacetic acid (EDTA, 5 mM) was added to the assay solution in the reactivation experiments to avoid further binding of the cofactor during the time of the measurement. To be able to acquire reliable kinetic data during the first 10 min of the reactivation process, aliquots from the refolding sample were withdrawn and incubated in the assay solution. In a control experiment, incubated and nonincubated refolding samples, withdrawn at the same time points during the first 10 min of refolding, exhibited identical activity. Reference samples that were identical in protein and GuHCl concentration and buffer solution to the refolding samples were used to correct for possible inhibition by GuHCl.

CD Measurements. Circular dichroism spectra and kinetic traces were recorded on a CD6 spectrodichrograph (Jobin-Yvon Instruments SA). The instrument was calibrated with an aqueous solution of *d*-10-(+)-camphorsulfonic acid. For equilibrium measurements of the protein variants, the near-UV CD spectra were recorded between 240 and 320 nm by collecting data at 0.5 nm intervals with an integration time of 2 s. In the equilibrium unfolding experiments, near-UV CD spectra were recorded to ensure that the spectral bands vanished uniformly during the unfolding process. From the spectra, the change in ellipticity at 270 nm ($[\theta]_{270}$) was observed; each spectrum (and data at 270 nm) represents the average of three scans and is subject to a mutual comparison before summation to detect possible alterations of the sample during the scanning period. In the refolding experiments, both near-UV CD spectra and kinetic CD traces were recorded. The kinetic CD traces were measured at 270 nm ($[\theta]_{270}$) by collecting data with an interval of 5 s and an integration time of 4.99 s. In addition, refolding experiments were also performed by recording near-UV CD spectra (260−310 nm, integration time of 2 s) during the refolding process at 4 min intervals from the onset of the data recording. Data collection, for both spectra and kinetic traces, was started 20 s after the onset of the refolding reaction and continued for at least 3 h. The kinetic experiments were recorded three times for each sample to ensure that the results were reproducible, and replicate refolding gave almost identical results. Measurements were performed using a 10 mm quartz cell while the temperature was maintained at 23.0 °C during all CD measurements by a temperature-controlled cell holder. The CD signals from the cuvette and sample lacking the protein were subtracted from all recorded spectra and kinetic traces. The CD spectra were smoothed using the minimal filter included in the CD6 software (Savinsky-Golay).

The ellipticity is reported as the mean residue molar ellipticity ($[\theta]$, deg cm^2 $dmol^{-1}$) calculated from

$$[\theta] = [\theta]_{obs}(mrw)/10cl \quad (1)$$

where $[\theta]_{obs}$ is the ellipticity measured in degrees, mrw is the mean residue molecular weight (molecular weight of 29 000 and 260 amino acid residues), c is the protein concentration (in grams per milliliter), and l is the optical path length of the cell (in centimeters).

Fluorescence Measurements. All fluorescence data were recorded on a Hitachi F-4500 spectrofluorophotometer using

Table 1: Kinetic Parameters[a] from Refolding Experiments Monitored as the Change in Tryptophan Fluorescence Quenching, Circular Dichroism, and CO_2 Hydration Activity

	tryptophan fluorescence quenching				CD at 270 nm				CO_2 hydration activity			
protein	k_1 ($\times 10^3$ s^{-1})	k_2 ($\times 10^3$ s^{-1})	A_1 (%)	A_2 (%)	k_1 ($\times 10^3$ s^{-1})	k_2 ($\times 10^3$ s^{-1})	A_1 (%)	A_2 (%)	k_1 ($\times 10^3$ s^{-1})	k_2 ($\times 10^3$ s^{-1})	A_1 (%)	A_2 (%)
Zn(II)	–	–	–	–	0.72 ± 0.04	0.17 ± 0.08	54 ± 2	46 ± 2	2.2 ± 1.7	0.34 ± 0.09	22 ± 13	72 ± 11
Co(II)	3.6 ± 0.48	0.38 ± 0.03	39 ± 3	61 ± 3	0.48 ± 0.04	0.23 ± 0.03	66 ± 11	34 ± 11	8.1 ± 2.5	0.37 ± 0.03	18 ± 3	82 ± 2

[a] The rate constants are mean values with standard deviations and are based on at least three refolding experiments.

a 10 mm quartz cuvette. The sample temperature was kept at 23.0 °C with a circulating water bath. In all experiments, the samples were excited at 295 nm. For the equilibrium unfolding measurements, the bandwidths for excitation and emission were both set to 5 nm, and the emission spectra were collected between 310 and 450 nm. Each spectrum is the average of three consecutively acquired spectra. All spectra were corrected by subtracting the spectrum of the blank, lacking the enzyme but otherwise identical to the sample, and smoothed using the filter included in the Hitachi F-4500 software.

For the refolding kinetic measurements, the sample was continuously excited at 295 nm and the emission intensity was collected at 340 nm with a response time of 8.0 s. The slits for the excitation and emission light were set to 5 and 2.5 nm, respectively. The data collection during the refolding process was initiated 20 s after the onset of the refolding reaction and continued for at least 3 h. The kinetic experiment was carried out three times to ensure that the results were reproducible, and replicate refolding gave almost identical results.

Fluorescence spectra of ANS were recorded from protein samples containing 8.5 μM protein and 410 μM ANS in 1.2 M GuHCl and 0.1 M Tris-H_2SO_4 (pH 7.5). Excitation of the sample was at 360 nm, and the fluorescence spectra were recorded between 380 and 600 nm using 10 nm slits for excitation and 5 nm slits for emission light.

Data Analysis. The reactivation data obtained from CD, fluorescence, and CO_2 hydration measurements were fitted to the sum of one- or two-exponential terms using the least-squares fitting option included in the program TableCurve 2D (Jandel Scientific).

The kinetic results (Table 1) represent the average of three repeated experiments.

The data from the equilibrium unfolding experiments, measured by intrinsic fluorescence and near-UV CD, were fitted to a nonlinear least-squares analysis described previously by Santoro and Bolen (*26*) using the program TableCurve 2D. A linear dependence of the free energy of unfolding on the GuHCl concentration was assumed in both transitions (*27*):

$$\Delta G = \Delta G^{H_2O} - m[\text{GuHCl}] \qquad (2)$$

The GuHCl concentration, C_m, in the midpoint of each of the unfolding transitions was determined from the ratio $\Delta G^{H_2O}/m$, when $\Delta G = 0$ (eq 2).

RESULTS AND DISCUSSION

Choice of Enzyme. We chose to use bovine CA II (BCA II) instead of human CA II (HCA II), even though the refolding properties of the latter have been more thoroughly studied (*28*). There were two main reasons for this choice, both essential for this study: (1) the molten globule intermediate of HCA II is very prone to aggregation (*29*), this problem being less pronounced for the BCA II intermediate, which facilitated our study involving this intermediate; and (2) cloned HCA II coordinates Co(II) not only to the active site but also to other binding sites, according to an analysis of the visible absorption spectrum (data not shown). Since various N-terminally truncated variants of HCA II do not seem to bind additional Co(II), the metal ion probably binds to the N-terminus, which has several potential His ligands. Moreover, erythrocyte HCA II appears to bind Co(II) only to the active site (*30*), indicating that the structural changes in the N-terminus of cloned HCA II (nonacetylated Ala instead of acetylated Ser) (*31*) play a role in this extra metal ion binding. Since our study focuses on the binding of Co(II) as a means of initiating the refolding reaction, the specific stoichiometric coordination of Co(II) to the active site of BCA II (*23*, *32*) represents yet another advantage of using this enzyme.

Equilibrium Unfolding of the BCA II Variants. Via measurement of the change in the stability of the protein structure during exposure to increasing concentrations of a denaturant, it is possible to observe cooperative transitions between different thermodynamic states of the protein structure. Monitoring this cooperative change in stability using different techniques, each probing different structural properties, provides a more detailed description of the structural changes occurring between the thermodynamic states.

Previous studies of denaturation profiles for apo-, Co(II)-, and Zn(II)-BCA II obtained using different denaturants and monitoring techniques have demonstrated the varying stability of the different forms of BCA II (*2*, *3*, *33*). It has also been demonstrated that the unfolding of apo-, Zn(II)-, and Co(II)-BCA II in GuHCl at room temperature is a three-state process, with the formation of a folding intermediate (molten globule) (*2*, *33*). Therefore, the aim of our stability experiments of the various cofactor forms of BCA II was to find denaturing conditions that might enable a refolding jump from the intermediate state (molten globule) of the apoenzyme to the native holoenzyme simply by adding the cofactor to initiate the process.

The stability of the BCA II variants against GuHCl denaturation was monitored by measuring near-UV CD, intrinsic tryptophan fluorescence, and CO_2 hydration activity to probe different structural aspects of the unfolding process. Only the first unfolding transition of the protein variants of BCA II, i.e., from the native to the molten globule state (N $\leftrightarrow$ I), was analyzed in detail. The near-UV CD unfolding could only detect the transition from the native to the molten globule state (Figure 1A), since the tertiary interactions are

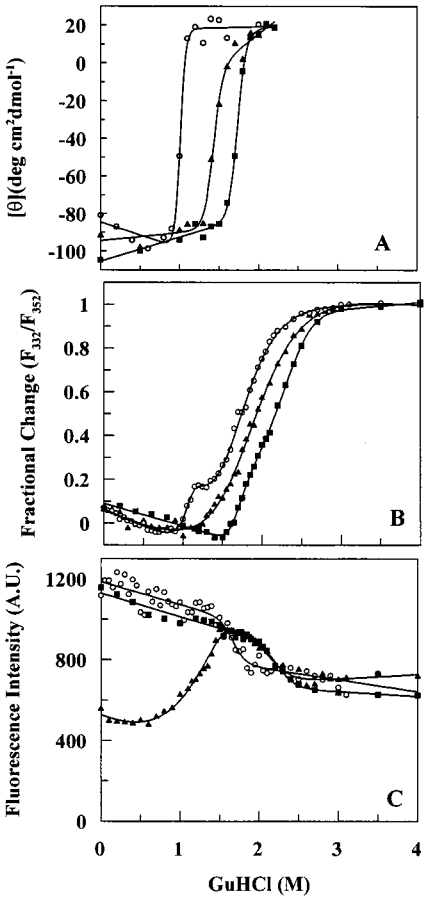

FIGURE 1: Stability curves of apo- and metalloenzyme forms of BCA II. (A) Change in near-UV CD ellipticity at 270 nm. (B) Fractional change in intrinsic Trp fluorescence, presented as ratios of the intensities at 332 and 352 nm. (C) Change in emission intensity at the fluorescence peak. Symbols: (○) apo-BCA II, (▲) Co(II)-BCA II, and (■) Zn(II)-BCA II.

broken in the molten globule state (*34*, *35*). However, the existence of a second unfolding transition, i.e., from the molten globule to the unfolded state (I ↔ U), was detected by intrinsic fluorescence measurements (Figure 1B).

CD Measurements. The near-UV CD bands of proteins mainly originate from the tertiary structure asymmetrically formed around aromatics, especially Trp side chains (*36*). This has clearly been demonstrated for carbonic anhydrase (*37*, *38*). The changes in ellipticity at 270 nm for the protein variants incubated in various concentrations of GuHCl were used to construct the stability profiles (Figure 1A). The near-UV CD ellipticity at 270 nm corresponds to the spectral minimum in the near-UV CD spectrum of the native form of the protein variants (Figure 2A,B). Thus, any spectral changes at this wavelength will mainly reflect a loss of local asymmetric tertiary structure surrounding the aromatic residues, especially the Trp residues. BCA II contains seven Trp residues, all of which are conserved in the bovine and human forms of the enzyme (*6*, *39*). When the arrangement in HCA II is considered, these seven Trp residues should be rather evenly distributed in the structure (*9*). Therefore, measurements of the change in ellipticity should reflect overall conformational changes rather well. According to the recorded CD spectra and associated unfolding curve (Figure 1A), tertiary structural interactions do not appear to remain in the molten globule state. During unfolding, the change in ellipticity of the positive CD band (at 245 nm) coincided

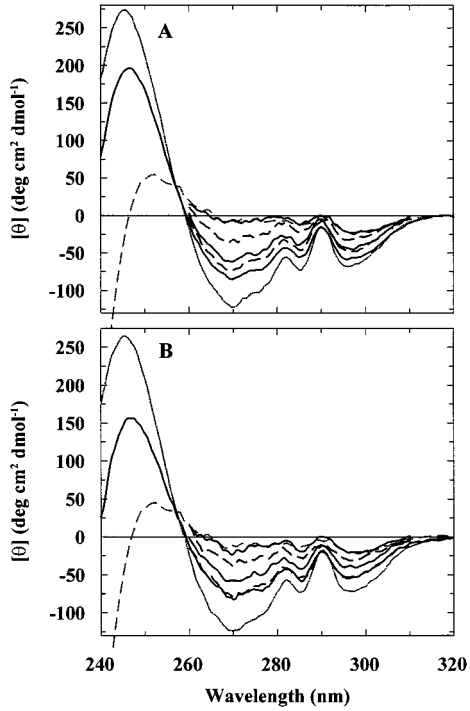

FIGURE 2: Development of near-UV CD spectra during refolding from the molten globule to the native state. Refolding was initiated by adding an equimolar amount of the metal cofactor to the apoenzyme in 1.2 M GuHCl. (A) Zn(II)-BCA II. References: apoenzyme in 1.2 M GuHCl (uppermost dashed curve) and the Zn-(II)-enzyme in 1.2 M GuHCl (lowest solid curve). (B) Co(II)-BCA II. References: apoenzyme in 1.2 M GuHCl (uppermost dashed curve) and the Co(II)-enzyme in 1.2 M GuHCl (lowest solid curve). Refolding times for both panels were 1 min, 20 min, 1 h, 2 h, and 3 h; the corresponding spectra were drawn with alternating solid and dashed lines in descending order. Identification of the curves applies to the wavelength region of 260−320 nm.

with that of the 270 nm band (data not shown), indicating that there is a uniform spectral change within the entire spectral region. That is, the observed spectral change during equilibrium unfolding can be regarded as a two-state process with no detectable intermediates between the native and the molten globule states.

The transition profiles (Figure 1A) from the unfolding transitions (N ↔ I) clearly show the influence of the cofactors on the stability of the native conformation. Calculated transition midpoint concentrations (C_m) from fitted (two-state) stablity curves gave the following results: Zn(II) was the most stabilizing cofactor, with a C_m of ∼1.7 M for Zn-(II)-BCA II compared to ∼1.4 and ∼1.0 M for Co(II)- and apo-BCA II, respectively. These values are very similar to those previously reported by Henkens et al. (*2*), who obtained the following C_m values for the first transition: 1.1, 1.5, and 1.8 M GuHCl for apo-BCA II, Co(II)-BCA II, and Zn(II)-BCA II, respectively.

It is obvious from Figure 1A that at 1.2 M GuHCl, it might be possible to perform a refolding jump from the molten globule state of the apoenzyme to the native state of either the Zn(II)- or Co(II)-enzyme. Such a transition could be monitored by CD measurements. The possibility exists because at that GuHCl concentration (1) the apoenzyme is in the intermediate (molten globule) state and not involved in the transition region and (2) both the Zn(II)- and Co(II)-enzymes are in the native state and are not involved in the transition region.

Tryptophan Fluorescence Measurements. The equilibrium unfolding was also monitored by measuring the intrinsic Trp fluorescence spectra of the three BCA II variants that were studied (Figure 1B). Like the near-UV CD changes, the changes observed in the emission spectra, when exciting the seven Trp residues of the protein at 295 nm, can be assumed to reflect global unfolding of the structure. The calculated ratios of the fluorescence intensities at 332 and 352 nm (F_{332}/F_{352}) indicate the exposure of buried Trp residues to a polar environment (*40*, *41*).

The equilibrium unfolding profiles (N → I and I → U) are illustrated in Figure 1B, in which the fractional change F_{332}/F_{352} is plotted versus GuHCl concentration. The solid lines in Figure 1B represent a nonlinear least-squares fit to two consecutive two-state transitions (three-state model), calculated by using a modification of the two-state model equation described by Santoro and Bolen (*26*), with the assumption that the free energy of folding is linearly dependent on the GuHCl concentration (*27*).

The unfolding transitions of the Zn(II)- and Co(II)-enzyme exhibited no marked plateau for the intermediate state. This lack of an apparent stable intermediate state can be explained by the narrowness of the midpoint GuHCl concentrations of the two transitions (*2*, *42*, *43*). The estimated C_m values for the first transition (N ↔ I) of the three protein variants are, despite the absence of an apparent intermediate, very similar to the corresponding values measured by CD [∼1.0, ∼1.5, and ∼1.8 M for apo-BCA II, Co(II)-BCA II, and Zn(II)-BCA II, respectively]. The unfolding of the apoenzyme from the native to the molten globule state at 1.2 M GuHCl was accompanied by a ∼2.5 nm (341.3 → 343.7 nm) red shift of the wavelength of the emission maximum. This minor shift in wavelength, compared to ∼13 nm for the "complete" unfolding of the native conformation in 4.0 M GuHCl, indicates that the Trp residues do not undergo any major changes in their exposure to the solvent in the transition to the molten globule state. This suggests a compact and only partially disturbed structure around the Trp residues. At 1.2 M GuHCl, the Zn(II)- and Co(II)-enzyme did not show any significant shifts in the wavelengths of the emission maxima compared to those obtained at 0 M GuHCl (data not shown). Accordingly, the F_{332}/F_{352} ratio did not change at 1.2 M GuHCl for the holoenzymes as demonstrated in Figure 1B. All together, the fluorescence data clearly show that the native structure of both the Zn(II)- and Co(II)-enzymes is maintained when exposed to this GuHCl concentration.

Interestingly enough, the unfolding transitions from the molten globule state to the unfolded state occurred at higher GuHCl concentrations for the metalloenzymes than for the apoenzyme, the molten globule of the Zn(II)-BCA II being the most stable intermediate (Figure 1B). The fact that the metal ion has an effect on the second unfolding transition has also been noted by Henkens et al. (*2*). We can therefore conclude that the metal ion not only stabilizes the native state relative to the molten globule state but also increases the stability of the molten globule state of BCA II as compared to the unfolded state. This demonstrates that the cofactor, Zn(II) or Co(II), is also bound to the molten globule state of the protein. By applying a thermodynamic cycle calculation, Hunt et al. (*44*) found indirect evidence that the molten globule of human CA II also binds the metal cofactor with considerable affinity [$K_D \sim 100$ pM and 0.25 μM for Zn(II) and Co(II), respectively]. However, the estimated dissociation constants for the molten globule of human CA II and the metal ions could differ significantly from the corresponding dissociation constants for BCA II used in this study.

Due to its paramagnetic character, Co(II) can efficiently quench emitted light, if it is located close enough to the emitter (*45*), Trp residues in this case. We measured the change in emission intensity during equilibrium unfolding of the Co(II)-enzyme (Figure 1C) to investigate the quenching effect of Co(II). This was done to determine whether the binding of Co(II) to the active site of the apoenzyme could be used as a probe to monitor structural changes close to the binding site of the metal ion during folding.

The following discussion of fluorescence quenching and energy transfer in BCA II is based on the crystal structure (*9*) and previous fluorescence studies (*41*) of HCA II, since the structures of BCA II and HCA II are assumed to be almost identical. Trp209 is located close to the active site and is fully quenched in the native state of HCA II, and this quenching is assumed to occur also in BCA II. This quenching is attributed to the proximity of Trp209 to the metal ligand His119 and also to His107. In addition, Trp209 quenches neighboring Trp192 by an energy transfer system. The fluorescence quenching effect of the Co(II) ion in BCA II was previously attributed to Trp209 (*2*). In light of our results, this interpretation seems less likely, since the native apoenzyme and the native Zn(II)-enzyme have identical fluorescence intensities (at 0 M GuHCl; Figure 1C), and therefore, Trp209 should already be fully quenched in the apoenzyme. The native Co(II)-enzyme, on the other hand, has only 50% of the fluorescence intensity of the native Zn(II)-enzyme and the apoenzyme (Figure 1C). Therefore, it is evident that the observed additional quenching in Co-BCA II, caused by the paramagnetic Co(II), must be attributed to Trp residues other than Trp209. In HCA II, Trp97 has been found to contribute 52% of the intrinsic fluorescence intensity of the enzyme (*41*). It is interesting to note that Trp97 is located next to one of the metal ligands, His96, in the active site of the protein and 10 Å from the metal ion. Thus, it is likely that the observed quenching of Co(II) in Co-BCA II can be attributed to Trp97 and possibly also to Trp245. The latter contributes 38% of the fluorescence intensity of HCA II and is located 11 Å from the metal ion. This quenching effect of Co(II), when bound to the active site of the protein, can be used as a sensitive probe to monitor structural changes in the residues directly or indirectly involved in the quenching mechanism.

The increase in intensity [i.e., the decrease in the level of Co(II) quenching] of the Trp fluorescence of Co(II)-BCA II accompanying the N → I transition (Figure 1C) appears to begin at ∼0.7 M GuHCl and peaks at 1.5 M GuHCl. The lower starting value of this transition compared to that observed from the CD measurements is due to lower concentrations of the protein and the metal ion in the fluorescence emission measurements (0.85 vs 8.5 μM). At 10-fold higher protein and metal ion concentrations, the corresponding change in fluorescence intensity starts at ∼1.2 M GuHCl and the transition has a midpoint at ∼1.4 M GuHCl (data not shown). Thus, the observed difference in stability as monitored by fluorescence intensity is only apparent and does not represent a conformational change

prior to global unfolding. The peak value at ~1.5 M GuHCl shows the end of further Co(II) quenching, reflecting a disruption of the compact metal-binding region and the molten globule intermediate indicated by the CD change reached at this GuHCl concentration (Figure 1A). The decrease observed in the fluorescence intensity for all the protein variants at higher GuHCl concentrations (Figure 1C) is probably due to an increased level of solvent exposure of the Trp residues upon further unfolding with an accompanying external quenching by water and solvent components. The resulting curve probably shows the second unfolding transition from the molten globule to the unfolded state.

Activity Measurements. We have previously reported equilibrium GuHCl denaturations of Zn(II)- and Co(II)-BCA II, measured as CO_2 hydration activity (*3*). Our present measurements show that the activity of the holoenzymes [Zn(II)-BCA II and Co(II)-BCA II] is not affected by incubation for 24 h with 0 and 1.2 M GuHCl [buffered with 0.1 M Tris-H_2SO_4 (pH 7.5)]. Thus, exposing the holoenzymes to 1.2 M GuHCl will probably have no significant effect on the native conformation.

ANS Binding and Fluorescence. The hydrophobic dye ANS is frequently used to identify the molten globule state (*46*, *47*). This state is compact and often has solvent-exposed hydrophobic surfaces to which ANS can bind, leading to a blue-shifted emission spectrum of ANS with increased intensity (*48*). Addition of ANS to Co(II)- and Zn(II)-BCA II in 1.2 M GuHCl did not lead to any change in the emission spectrum compared to that of ANS dissolved in 1.2 M GuHCl (Figure 4). However, ANS binding to the apoenzyme incubated in 1.2 M GuHCl resulted in a pronounced increase in the fluorescence intensity and a 40 nm blue shift of the emission wavelength maximum to 478 nm (Figure 4). This fluorescence spectrum is typical of ANS bound to the molten globule state.

Properties of the Intermediate State of the Apoenzyme and the Holoenzyme at 1.2 M GuHCl. The intermediate state of the apoenzyme at 1.2 M GuHCl seems to fit the description of the molten globule state of BCA II (*43*), showing the following characteristics: (i) the lack of tertiary interactions, at least locally around the Trp residues, as judged from the near-UV CD spectra; (ii) maintenance of secondary structure (far-UV CD, data not shown); (iii) the presence of a compact dehydrated structure with only a minor increase in the level of solvent exposure of the Trp residues, as suggested by the intrinsic Trp fluorescence measurements; and (iv) exposure of hydrophobic patches, as indicated by ANS binding.

The properties of the holoenzymes after incubation in 1.2 M GuHCl are as follows: (i) intact tertiary structure, at least around the Trp residues, according to near-UV CD spectra and the intrinsic fluorescence shift; (ii) intact secondary structure according to far-UV CD spectra (data not shown); (iii) full activity, indicating an intact active site region; and (iv) no exposure of hydrophobic patches, based on ANS fluorescence.

Cofactor-Induced Refolding of the Apo Molten Globule to the Native State. Both fluorescence (Figure 1B) and CD (Figure 1A) measurements clearly show that cofactor-induced folding jumps from the molten globule state of the apoenzyme to the native state of both the Zn(II)- and Co(II)-enzymes should be possible at 1.2 M GuHCl. The measurements also indicate that the refolding process can be monitored by these parameters, which probe different aspects of the folding process. The reason for applying the cofactor strategy when refolding BCA II is that refolding from an intermediate (molten globule) state to the native state can be studied without changing the denaturing medium and, more specifically, that effects induced by the cofactor can be monitored.

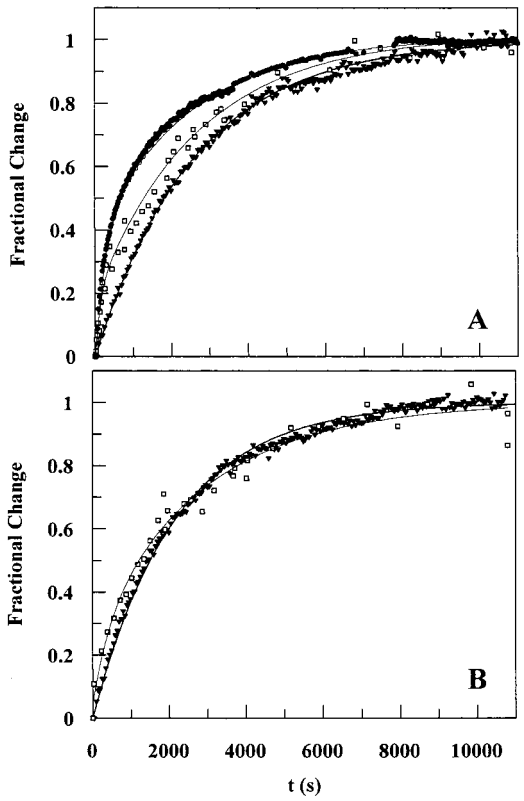

FIGURE 3: Cofactor-induced refolding of BCA II from the molten globule state. Refolding was initiated by adding an equimolar amount of the metal cofactor to the apoenzyme in 1.2 M GuHCl. (A) Co(II)-BCA II: (●) quenching of Trp fluorescence at 340 nm, (□) recovery of enzyme activity, and (▼) change in ellipticity at 270 nm. (B) Zn(II)-BCA II: (□) recovery of enzyme activity and (▼) change in ellipticity at 270 nm. The curves in both panels were obtained after fitting to the sum of two-exponential terms.

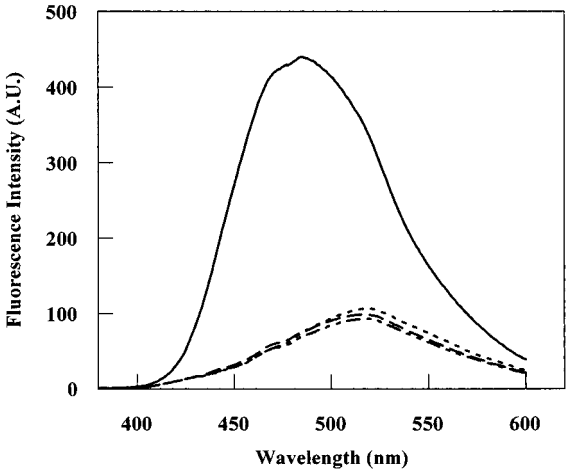

FIGURE 4: Fluorescence of ANS upon binding to various forms of BCA II: (—) ANS and apo-BCA II, (— — —) ANS and Co(II)-BCA II, (— - - —) ANS and Zn(II)-BCA II, and (- - -) ANS. All samples were incubated in 1.2 M GuHCl.

Initially, we investigated the amount of time needed to convert the apoenzyme to the molten globule intermediate in the presence of 1.2 M GuHCl. We found that apo-BCA II exhibited no change in the near-UV CD and intrinsic Trp fluorescence spectra after 1 h at this GuHCl concentration. The apoenzyme was thereafter incubated in 1.2 M GuHCl for 3 h with an equimolar amount of cofactor, and the state of the protein was subsequently analyzed to see whether the properties lost in the molten globule state could be regained by adding the cofactor. The different analytical methods gave the following recoveries of native protein when initiating the refolding process with Zn(II) or Co(II): near-UV CD, 67% Zn(II) and 61% Co(II); enzymatic activity, 91% Zn(II) and 82% Co(II); and quenching of the intrinsic Trp fluorescence, 81% Co(II). Thus, most of the native characteristics can, indeed, be regained solely by adding the cofactor under these experimental conditions. The differences in recoveries registered with the methods that were used were probably due to different interfering effects of a misfolded population, because aggregation has been shown to occur to some extent during the refolding of BCA II (*49*, *50*). In the following kinetic measurements, two reference samples were used to define the intial and final values for the refolding process: the apoenzyme incubated for 1 h in 1.2 M GuHCl (initial value) and the holoenzymes incubated in 1.2 M GuHCl for at least 2 h (final value).

Refolding Studied by CD Measurements. The near-UV CD spectrum of a protein is a sensitive measure of the conformation, revealing changes in native tertiary structure, and can therefore be used to "fingerprint" the native conformation of the protein (*51*, *52*). Thus, changes in the near-UV CD spectrum of a protein can be used to monitor the reattainment of the native tertiary conformation during refolding, as has been shown for HCA II (*53*). The refolding process from the molten globule to the native state of the protein was monitored by either the change in ellipticity at 270 nm or the change in the entire near-UV spectrum. Figure 2 shows that, at an early stage of the refolding process, the CD spectra acquired structural features quite similar to those of the native spectrum. An isodichroic point can be found at ~258 nm, indicating that the native tertiary structure was formed early and that no intermediate population was formed during the refolding process. The Co(II)- and Zn(II)-refolded apo molten globule appeared to have formed the native tertiary structure, since the spectral bands of the final CD spectra were very similar to those of the native holoenzymes. However, the ellipticities were somewhat higher, probably due to a minor population with misfolded structures.

Refolding Studied by Fluorescence Measurements. Measurements of the Trp fluorescence quenching during the Co(II)-induced refolding of the molten globule also showed that the structure of the Co(II)-enzyme was regained, indicated as successive quenching by Co(II).

As previously discussed, Co(II) is still bound in the molten globule intermediate of Co(II)-BCA II. The metal ion can, of course, also bind to the molten globule of the apoenzyme, since it can induce refolding. However, Co(II) binding to the molten globule in itself does not lead to fluorescence quenching, as revealed by the identical fluorescence intensities of the molten globules of the Co(II)- and Zn(II)-enzymes (at 1.8−2.0 M GuHCl; Figure 1C). Therefore, the quenching of Trp fluorescence by Co(II) reflects the formation of a compact metal-binding region, including the neighboring residues Trp97 and Trp245, which develops during refolding rather than during the binding process.

Kinetics of Co(II)-Induced Refolding of the Apo Molten Globule to the Native State. To investigate whether the kinetics of the structural rearrangements of the apoenzyme induced by Co(II) are affected by the concentration of the metal ion, the refolding kinetics were investigated after addition of an equimolar or a 5-fold molar excess of Co(II). The refolding kinetics were monitored by Trp fluorescence at 340 nm and the change in CD ellipticity at 270 nm. All these experiments were carried out five times with no observed differences in the time courses of the reactions when Co(II) and the apoprotein were present in a 1:1 or 5:1 ratio. This demonstrates that the processes that were investigated are first-order reactions, and it also suggests that the metal ion is rapidly bound to the enzyme initially. Subsequently, the protein undergoes conformational rearrangements, as observed in the structural and functional parameters that were employed.

Representative kinetic traces, appearing when the metal ion is added in an equimolar amount to the apoenzyme, are shown in Figure 3A. The reaction was monitored by the change in ellipticity at 270 nm, the quenching of tryptophan fluorescence, and the recovery of enzyme activity. For all the parameters that were studied, there were no further changes observed after 3 h of refolding, indicating that the refolding process is completed within this time. The kinetics of Co(II)-induced refolding were best fitted to the sum of two-exponential terms, suggesting a fast and a slow folding population in the initial folding state (i.e., the molten globule state of the apoenzyme). The rate constants and amplitudes are summarized in Table 1.

Comparison of the different kinetics of the various parameters gives a detailed picture of the pathway of the metal-induced refolding of BCA II from the apo molten globule to the native state. Considering the time courses shown in Figure 3A and the rate constants given in Table 1, we conclude that the quenching of tryptophan fluorescence occurs at the fastest rate, despite the fact that the initial phase of reactivation is the most rapid event. However, the low amplitude of the initial phase compared to that of the quenching of tryptophan fluorescence makes the total quenching faster. It is obvious that the slowest steps in the refolding reaction were recorded by near-UV CD.

Refolding from the molten globule state of BCA II can be outlined as follows. First, Co(II) binds to the molten globule and thereby initiates a compaction of the metal-binding region, detected as tryptophan quenching. Thereafter, formation of a native active site occurs, recorded as the recovery of enzyme activity. In a previous study of the refolding of completely denatured Co(II)-BCA II (*54*), we also found that Co(II)-binding intermediates were formed before a functioning active site was completed. The second of two Co(II) intermediates that were detected developed a native Co(II) spectrum, indicating that the final tetrahedral coordination of the metal ion had been established at this stage. The final folding steps involve formation of the native tertiary structure, seen as the reappearance of the near-UV CD spectral bands.

Kinetics of Zn(II)-Induced Refolding of the Apo Molten Globule to the Native State. Only two of the methods we

applied (near-UV CD and enzyme activity measurements) could be used to monitor Zn(II)-initiated refolding. Similar to the Co(II)-initiated refolding, the Zn(II)-induced refolding kinetics were independent of the concentration of the metal ion, since a stoichiometric amount of Zn(II) and a 5-fold molar excess of Zn(II) over enzyme gave rise to the same time courses when the reaction was assessed by CD. The kinetic traces for the refolding induced by an equimolar amount of Zn(II) registered by CD as well as by recovery of enzyme activity are shown in Figure 3B. As with the Co(II)-initiated refolding, the Zn(II)-induced refolding could be best fitted by the sum of two-exponential terms, suggesting a fast and a slow folding population. However, the regain of enzymatic activity seems to have a small burst phase. The rate constants and amplitudes are summarized in Table 1.

As for Co(II)-initiated refolding, the regain of enzyme activity when refolding was initiated by Zn(II) was somewhat faster than the reappearance of the near-UV CD spectrum, although the difference was not so marked with Zn(II).

Comparison of the Zn(II)- and Co(II)-Induced Refolding Kinetics. The rate constants observed from the cofactor-induced refolding are, in a strict sense, relaxation rate constants (i.e., $k_u + k_f$), because the measurements were carried out in the vicinity of the unfolding transition zone for the holoenzymes. On the other hand, in refolding experiments conducted under strongly native conditions, the observed rate constant became close to k_f (*27*). The somewhat slower refolding kinetics of the Co(II)-enzyme compared to that of the Zn(II)-enzyme, measured as near-UV CD at 270 nm (Table 1), are therefore consistent with the lower stability of the Co(II)-enzyme and also reflect the lower affinity of the apoenzyme for Co(II). It is more difficult to judge whether there is a difference in the kinetics of reactivation between the Co(II)- and Zn(II)-enzymes (Table 1), because the data are not as reliable as the CD data, due to difficulties incurred with obtaining accurate data in the initial phase of refolding. However, for both holoenzymes, formation of an enzymatically active structure seems to occur somewhat faster than formation of the final native tertiary conformation, especially for the Co(II)-enzyme. This suggests that a structure-possessing enzymatic activity is formed faster than the final tertiary structure, involving the entire protein molecule. A possible explanation for this could be that one or several structural regions in the outer part of the protein, which are not directly involved in the catalytic action of the enzyme, attain their final native structure somewhat slower than the active site core region does. Interestingly enough, for HCA II it has been demonstrated that a hydrophobic cluster close to metal ligands His94 and His96 is important for the Co(II) and Zn(II) affinity and possibly for orienting these His residues (*44*, *55*). This cluster has also been shown to be formed very rapidly in the refolding of HCA II (*56*). Co(II)-BCA II exhibited a greater difference between the kinetics of the regain of the near-UV CD and enzymatic activity compared to that observed for Zn(II)-BCA II. This might suggest that the lower global stability of the Co(II)-enzyme has a greater influence on the formation of the complete native tertiary structure than on the formation of a functioning active site.

Previously published results regarding refolding of fully GuHCl-unfolded BCA II have also shown that the Zn(II)- and Co(II)-enzymes have reasonably similar reactivation kinetics, with $t_{1/2}$ values of 9 and 12 min, respectively (*3*, *18*, *54*). Furthermore, Henkens et al. (*2*) noted that the kinetics of reactivation of the Zn(II)-enzyme either from the intermediate (molten globule) state or from the completely unfolded state had the same rate constants, suggesting that both processes have the same rate-limiting step. Semisotnov et al. (*17*) proposed that, when starting from either the fully unfolded or the intermediate state, the slow refolding process is due to slow isomerization of cis prolines. This was later confirmed in experiments demonstrating that proline isomerase catalyzes the reactivation of BCA II (*18*). Thus, the metal ion-induced reactivation of most of the molecules in the molten globule state, corresponding to the slow kinetic phase, seems to be limited by proline isomerization.

CONCLUSIONS

It is possible to induce refolding of the molten globule form of apo-BCA II merely by adding the metal ion cofactor of the enzyme. The refolding reaction from the molten globule to the native state can be summarized as follows: (i) initial binding of the metal ion to the molten globule state, (ii) compaction of the metal-binding region induced by the metal ion binding, (iii) formation of a functioning active site, and (iv) formation of the native tertiary structure. The final slow steps include adjustments of the structure in the outer part of the protein and cis−trans isomerization of proline residues.

REFERENCES

1. DeGrado, W. F., Summa, C. M., Pavone, V., Nastri, F., and Lombardi, A. (1999) *Annu. Rev. Biochem. 68*, 779−819.
2. Henkens, R. W., Kitchell, B. B., Lottich, S. C., Stein, P. J., and Williams, T. J. (1982) *Biochemistry 21*, 5918−5923.
3. Bergenhem, N., Carlsson, U., Lind, G., and Åstrand, I.-M. (1983) *Acta Chem. Scand. B37*, 244−246.
4. Lindskog, S. (1997) *Pharmacol. Ther. 74*, 1−20.
5. Nyman, P. O., and Lindskog, S. (1964) *Biochim. Biophys. Acta 85*, 141−151.
6. Sciaky, M., Limozin, N., Filippi-Foreau, D., Gullian, J.-M., and Laurent-Tabusse, G. (1976) *Biochimie 58*, 1071−1082.
7. Kannan, K. K., Notstrand, B., Fridborg, K., Lövgren, S., Ohlsson, A., and Petef, M. (1975) *Proc. Natl. Acad. Sci. U.S.A. 72*, 51−55.
8. Eriksson, E. A., Jones, A. T., and Liljas, A. (1988) *Proteins: Struct., Funct., Genet. 4*, 274−282.
9. Håkansson, K., Carlsson, M., Svensson, L. A., and Liljas, A. (1992) *J. Mol. Biol. 227*, 1192−1204.
10. Eriksson, E. A., and Liljas, A. (1993) *Proteins: Struct., Funct., Genet. 16*, 29−42.
11. Mårtensson, L.-G., Jonsson, B.-H., Freskgård, P.-O., Kihlgren, A., Svensson, M., and Carlsson, U. (1993) *Biochemistry 32*, 224−231.
12. Svensson, M., Jonasson, P., Freskgård, P.-O., Jonsson, B.-H., Lindgren, M., Mårtensson, L.-G., Gentile, M., Borén, K., and Carlsson, U. (1995) *Biochemistry 34*, 8606−8620.
13. Hammarström, P., Kalman, B., Jonsson, B.-H., and Carlsson, U. (1997) *FEBS Lett. 420*, 63−68.
14. Håkansson, K., Wehnert, A., and Liljas, A. (1994) *Acta Crystallogr. D50*, 93−100.
15. Dobson, C. M., and Karplus, M. (1999) *Curr. Opin. Struct. Biol. 9*, 92−101.
16. Semisotnov, G. V., Rodinova, N. A., Kutyshenko, V. P., Ebert, B., Blanck, J., and Ptitsyn, O. B. (1987) *FEBS Lett. 224*, 9−13.
17. Semisotnov, G. V., Uversky, V. N., Sokolovsky, I. V., Gutin, A. M., Razgulyaev, O. I., and Rodinova, N. A. (1990) *J. Mol. Biol. 213*, 561−568.

18. Fransson, C., Freskgård, P.-O., Herbertsson, H., Johansson, Å., Jonsson, P., Mårtensson, L.-G., Svensson, M., Jonsson, B.-H., and Carlsson, U. (1992) *FEBS Lett. 296*, 90−94.
19. Uversky, V. N., and Ptitsyn, O. B. (1995) *J. Mol. Biol. 255*, 215−228.
20. Nozaki, Y. (1972) *Methods Enzymol. 26*, 43−50.
21. Lindskog, S. (1960) *Biochim. Biophys. Acta 39*, 218−226.
22. Khalifah, R. G., Strader, D. J., Bryant, S. H., and Gibson, S. M. (1977) *Biochemistry 16*, 2241−2247.
23. Lindskog, S., and Malmström, B. G. (1962) *J. Biol. Chem. 237*, 1129−1131.
24. Hunt, J. B., Rhee, M.-J., and Storm, C. B. (1977) *Anal. Biochem. 72*, 614−617.
25. Rickli, E. E., Gazanfar, S. A. S., Gibbons, B. H., and Edsall, J. T. (1964) *J. Biol. Chem. 242*, 4206−4211.
26. Santoro, M. M., and Bolen, D. W. (1988) *Biochemistry 27*, 8063−8068.
27. Schellman, J. A. (1978) *Biopolymers 17*, 1305−1322.
28. Carlsson, U., and Jonsson, B.-H. (1995) *Curr. Opin. Struct. Biol. 5*, 482−487.
29. Hammarström, P., Persson, M., Freskgård, P.-O., Mårtensson, L.-G., Andersson, D., Jonsson, B.-H., and Carlsson, U. (1999) *J. Biol. Chem. 274*, 32897−32903.
30. Lindskog, S., and Nyman, P.-O. (1964) *Biochim. Biophys. Acta 85*, 462−474.
31. Nair, K. N., Calderone, T. L., Christianson, D. W., and Fierke, C. A. (1991) *J. Biol. Chem. 266*, 17320−17325.
32. Lindskog, S. (1963) *J. Biol. Chem. 238*, 945−951.
33. McCoy, L. F., and Wong, K.-P. (1979) *Biopolymers 18*, 2893−2904.
34. Dolgikh, D. A., Kolomiets, A. P., Bolotina, I. A., and Ptitsyn, O. B. (1984) *FEBS Lett. 165*, 88−92.
35. Borén, K., and Carlsson, U. (1999) *Biochim. Biophys. Acta 1430*, 111−118.
36. Strickland, E. H. (1974) *CRC Crit. Rev. Biochem. 2*, 113−175.
37. Freskgård, P.-O., Mårtensson, L.-G., Jonasson, P., Jonsson, B.-H., and Carlsson, U. (1994) *Biochemistry 33*, 14281−14288.
38. Borén, K., Freskgård, P.-O., and Carlsson, U. (1996) *Protein Sci. 5*, 2479−2484.
39. Henderson, L. E., Henriksson, D., and Nyman, P.-O. (1976) *J. Biol. Chem. 251*, 5457−5463.
40. Banik, U., Saha., R., Mandal, N. C., Battacharayya, B., and Roy, S. (1992) *Eur. J. Biochem. 206*, 15−21.
41. Mårtensson, L.-G., Jonasson, P., Freskgård, P.-O., Svensson, M., Carlsson, U., and Jonsson, B.-H. (1995) *Biochemistry 34*, 1011−1021.
42. Wong, K.-P., and Hamlin, L. M. (1975) *Arch. Biochem. Biophys. 170*, 12−22.
43. Ptitsyn, O. B. (1992) in *Protein Folding* (Creighton, T. E., Ed.) pp 243−300, W. H. Freeman and Co., New York.
44. Hunt, J. A., Ahmed, M., and Fierke, A. (1999) *Biochemistry 38*, 9054−9062.
45. Lakowicz, J. R. (1999) in *Principles of Fluorescence Spectroscopy*, pp 237−239, Kluwer Academic/Plenum Publishers, New York.
46. Ptitsyn, O. B., Pain, R. H., Semisotnov, G. V., Zerovnik, E., and Razgulyaev, O. I. (1990) *FEBS Lett. 262*, 20−24.
47. Semisotnov, G. V., Rodinova, N. A., Razgulyaev, O. I., Uversky, V. N., and Gilmanshin, R. I. (1991) *Biopolymers, 31*, 119−128.
48. Stryer, L. (1965) *J. Mol. Biol. 13*, 482−495.
49. Cleland, J. L., and Wang, D. I. C. (1990) *Biochemistry 29*, 11072−11078.
50. Wetlaufer, D. B., and Xie, Y. (1995) *Protein Sci. 4*, 1535−1543.
51. Woody, R. W. (1995) *Methods Enzymol. 246*, 34−71.
52. Kelly, S. M., and Price, N. C. (1997) *Biochim. Biophys. Acta 1338*, 161−185.
53. Andersson, D., Freskgård, P.-O., Jonsson, B.-H., and Carlsson, U. (1997) *Biochemistry 36*, 4623−4630.
54. Bergenhem, N., and Carlsson, U. (1989) *Biochim. Biophys. Acta 998*, 277−285.
55. Hunt, J. A., and Fierke, C. A. (1997) *J. Biol. Chem. 272*, 20364−20372.
56. Jonasson, P., Aronsson, G., Carlsson, U., and Jonsson, B.-H. (1997) *Biochemistry 36*, 5142−5148.

BI000957E